J Mol Model (2012) 18:2357–2367
DOI 10.1007/s00894-011-1258-2

ORIGINAL PAPER

Theoretical investigation of the two-photon absorption properties of 3,6-bis(4-vinylpyridinium) carbazole derivatives—new biological fluorescent probes

Ying Sun · Yang Zhao · Xiao-Ting Liu · Ai-Min Ren · Ji-Kang Feng · Xiao-Qiang Yu

Received: 17 April 2011 / Accepted: 22 September 2011 / Published online: 12 October 2011

Abstract The present study focuses on a series of carbazole derivatives, which are being investigated as potential two-photon fluorescent probes (TFP) for DNA detection and two-photon bioimaging. The geometric structures, electronic structures, and the one-photon (OPA) and two-photon (TPA) absorption properties of 3,6-bis(1-methyl-4-vinylpyridinium) carbazole (BMVC) derivatives, as well as their dications and diiodized derivatives, were studied using density functional theory (DFT) and Zerner's intermediate neglect of differential overlap (ZINDO) method. The results showed that the TPA spectra of the diiodized BMVC derivatives and their dications are all found in the near-infrared region (NIR). At the same time, the diiodized BMVC derivatives presented larger TPA cross-sections than the neutral BMVC derivatives and the dications. These theoretically derived values were also in good agreement with their corresponding experimentally observed values, and they indicated that the diiodized BMVC may be the form of this TFP that combines with DNA. The diiodized BMVC derivatives and the dications have the potential to be excellent TPA materials, especially when used as TFPs in nucleic acid imaging applications.

Keywords Iodized 3,6-bis(4-vinylpyridinium) carbazole derivatives · One-photon absorption · Two-photon absorption cross-section · Two-photon fluorescence probe · Density functional theory

Y. Sun · Y. Zhao · X.-T. Liu · A.-M. Ren (✉) · J.-K. Feng
State Key Laboratory of Theoretical and Computational Chemistry, Institute of Theoretical Chemistry, Jilin University, Changchun 130023, People's Republic of China
e-mail: aimin_ren@yahoo.com

X.-Q. Yu
State Key Laboratory of Crystal Materials, Shandong University, Jinan 250100, People's Republic of China

Introduction

Nonlinear optics (NLO) is a relatively new branch of optics. Half a century since the laser was first demonstrated—which led to the first explorations of NLO—the fundamental principles of NLO and applications of NLO materials have become hot research topics. Two-photon absorption (TPA) is a third-order nonlinear absorption process involving the simultaneous absorption of two either degenerate or nondegenerate photons. TPA has various applications, such as three-dimensional (3D) optical data storage [1, 2], 3D optical imaging for biological systems [3, 4], 3D micro-fabrication and early corrosion detection [5, 6], optical power limiting [7], and photodynamic therapy [8]. In recent years, researchers have paid great attention to the development of TPA materials for use in the life sciences. In particular, two-photon fluorescence microscopy (TPFM) has proven irreplaceable when there is a need to perform live biological tissue imaging without causing trauma [9–12]. TPFM has many characteristics; for instance, it produces high-contrast images, and it does not lead to `UV damage to biological samples, photobleaching, or fluorescent interference outside the focal plane [13–15], unlike traditional optical microscopy. However, TPFM requires highly sensitive TPA molecules, which presents a problem with biological applications of TFPM, as most known TPA molecules are not biocompatible, as they are often insoluble in water or are easily form nonfluorescent aggregates in solution. As a result, highly active two-photon excited fluorophores for DNA are rather rare. Therefore, designing and synthesizing suitable two-photon fluorescent probe (TFP) materials is an attractive line of research. Very recently, Yu et al. synthesized a series of compounds named 3,6-bis(4-vinylpyridinium) carbazole derivatives, which exhibit good TPA properties and are potentially efficient TFPs for DNA [16]. However, the

electronic structure of these TFPs and their intrinsic interactions with DNA remain unclear. In this work, we designed a series of TFP molecules based on 3,6-carbazole derivatives. Their one-photon absorption (OPA) spectra, their TPA spectra, and the relationship between the structures of the studied molecules and their one- and two-photon absorption properties were studied theoretically. Comparing these calculated TPA spectra to the corresponding experimental data [16], we were able to identify the actual form of the 3,6-carbazole derivatives that combines with DNA. This research should provide useful theoretical guidelines for designing and synthesizing new TPA fluorescence probes with excellent TPA properties.

Computational methods

The TPA process involves the simultaneous absorption of two photons. The TPA efficiency of an organic molecule for an optical frequency $\omega/2\pi$ can be characterized by the TPA cross-section $\delta(\omega)$. This can be directly related to the imaginary part of the third-order polarizability $\gamma(-\omega;\ \omega,\ -\omega,\ \omega)$ [17, 18], as shown in the following equation:

$$\delta(\omega) = \frac{3\hbar\omega^2}{2n^2c^2\varepsilon_0} L^4 \mathrm{Im}[\gamma(-\omega;\omega,-\omega,\omega)], \tag{1}$$

where $\gamma(-\omega;\ \omega,\ \omega,\ -\omega)$ is the third-order polarizability, $\hbar\omega$ is the energy of the incoming photons, c is the speed of light, ε_0 is the electric permittivity in a vacuum, n denotes the refractive index of the medium, and L corresponds to the local-field factor. In the calculations presented here, n and L are set to 1 because we will consider isolated molecules in a vacuum.

The sum-over-states (SOS) expression, which is used to evaluate the components of the third-order polarizability $\gamma(-\omega;\ \omega,\ -\omega,\ \omega)$, can be deduced using perturbation theory. If we consider a Taylor expansion of the energy with respect to the applied field, the $\gamma_{\alpha\beta\gamma\delta}$ Cartesian components are given in [19, 20].

To compare the calculated δ value with the experimental value [16] measured in solution, the orientationally averaged (isotropic) value of γ is evaluated, which is defined as

$$\langle\gamma\rangle = \frac{1}{15}\sum_{i,j}\left(\gamma_{iijj} + \gamma_{ijij} + \gamma_{ijji}\right) \qquad i,j = \mathrm{x,y,z}. \tag{2}$$

In the present paper, the ground-state equilibrium geometries of all molecules were optimized using the DFT/B3LYP method, combining the 6-31+G(d) basis set for the C, O, N, and H atoms with the DGDZVP basis set for iodine atoms [21] in the Gaussian03 program [22]. Then, based on the optimized geometries, one-photon absorption (OPA) spectra were calculated by the TDDFT//B3LYP/6-31+G (d) and ZINDO methods, respectively. The state dipole moment, transition dipole moment, and transition energy were obtained by a single- and double-electron excitation configuration interaction approach employing the ZINDO method [23, 24]. For all molecules, the CI-active spaces were restricted to the 30 highest occupied and 30 lowest unoccupied molecular orbitals for the singly excited configuration and the two highest occupied and two lowest unoccupied orbitals for the doubly excited configuration. The ZINDO method is often employed to investigate one- or two-photon properties as it provides a better description of the lowest-lying excited states for large organic molecules or practical organic molecules than ab initio methods and first-principles DFT [25, 26]. We set up the FTRNLO program to calculate the third-order polarizability γ and the TPA cross-section δ, based on to Eqs. 1 and 2. An effective approach was used to obtain the two-photon absorption that involved combining the SDCI method with the SOS formulae [21, 24, 27–30] and Eqs. 1 and 2 in the ZINDO program.

Results and discussion

Molecular design and geometry optimization

Experimental research has confirmed that 3,6-bis(4-vinylpyridinium) carbazole derivatives are potentially a type of TFP [16]. However, the micromechanism of the interaction between the structure of this type of TFP and DNA has not yet been explained. Owing to the polarity of the water, the variety of hydrophilic and hydrophobic properties of DNA, and the iodine ions intrinsically present in the biological system, the form of the fluorescent probe (ionized, neutral, or iodized) that is loaded into biological tissues and combines with DNA is as yet unclear. To investigate the actual form of the probe that interacts with DNA, we designed a series of TFP molecules (as shown in Fig. 1) based on the 3,6-carbazole derivatives.

The chemical structures of the 3,6-bis(4-vinylpyridinium) carbazole (BVC) derivatives considered in this work are shown in Fig. 1 [31]. In order to study the effects of the substituents on the TPA properties of these derivatives, a series of 3,6-bis(1-methyl-4-vinylpyridinium) carbazole (BMVC) derivatives were designed with substituents of different sizes at the 9 position. At the same time, we also designed a series of 3,6-bis(1-methyl-4-vinylpyridinium) carbazole dication (BMVC-C) derivatives and iodized 3,6-bis(1-methyl-4-vinylpyridinium) carbazole (BMVC-I) derivatives (as shown in Fig. 1), in order to investigate how charge

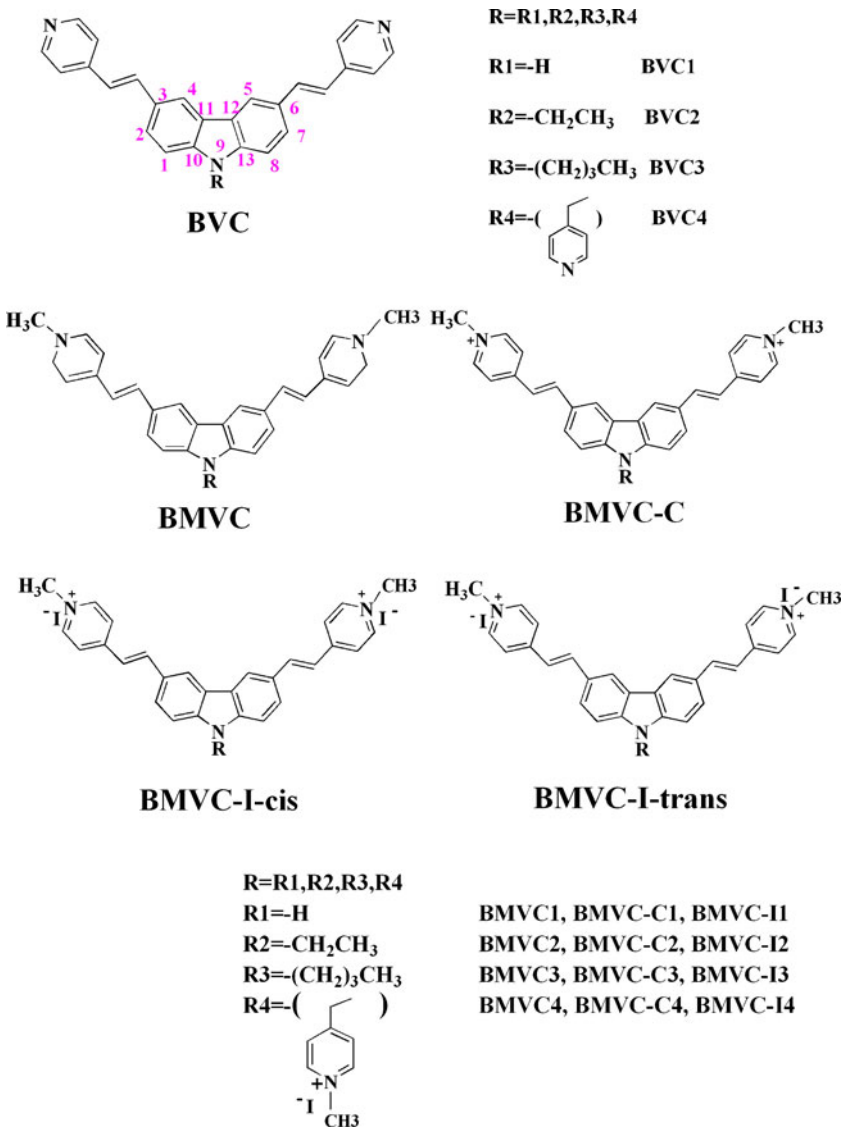

Fig. 1 Chemical structures of all of the molecules studied. BVC: 3,6-bis(4-vinylpyridinium) carbazole. BMVC: 3,6-bis(1-methyl-4-vinylpyridinium) carbazole. BMVC-C: 3,6-bis(1-methyl-4-vinylpyridinium) carbazole dication. BMVC-I: diiodized 3,6-bis(1-methyl-4-vinylpyridinium) carbazole

and the presence of iodine ion affect the electronic structures and TPA properties of the derivatives.

For the BMVC-I1 and BMVC-I2 molecules of the BMVC-I series, when the two iodine ions are on the same side of the BMVC derivative when viewed in the direction of one pyridinium group from the other pyridinium group, the molecule is termed the *cis*-BMVC-I isomer; if the two iodine ions are on opposite sides, the molecule is termed the BMVC-I-*trans* isomer. We compared the total molecular energies (calculated by DFT) of the two resulting series of isomers in order to evaluate their stabilities. The energy of BMVC-I1-*cis* with the R1 substituent is 3.8 kcal mol^{-1} less than that of BMVC-I1-*trans*, and the energy of BMVC-I2-*cis* with the R2 group is 2.8 kcal mol^{-1} less than that of BMVC-I2-*trans*. These results indicate that the *cis* isomers are more stable than the *trans* isomers. Frequency calculation results for the *cis*-BMVC-I molecules with R1 and R2 substituents indicate that they have no imaginary frequencies. Therefore, we will consider the *cis* isomers rather than the *trans* isomers in the following discussion.

The B3LYP/6-31+G (d) method was used to obtain the stable ground geometries of the molecules. The dihedral angle between the central carbazole ring and the vinyl group in the BMVC and BMVC-C molecules was found to be close to 180°. However, this dihedral angle changed to 3.7° when position 9 received R4 as a substituent. In addition, for BMVC-I1, BMVC-I2 and BMVC-I3, the dihedral angle between the vinyl groups at the 3 and 6 positions and the central carbazole ring is about 12.6°, and exhibits obvious distortion. The dihedral angle between the substituents at the 3, 6, and 9 positions and the central carbazole ring of molecule BMVC-I4 is about 9.0°. Such small distortions (3–13°) can be overcome when the molecules combine with DNA, so they would not prevent

these molecules from yielding high quantum efficiencies and being used as DNA molecular "light switches" [16].

One-photon absorption properties

First, based on the optimized geometry structures obtained at the B3LYP/6-31+G (d) level, the OPA properties were investigated using both ZINDO and TDDFT methods. The wavelength of maximum OPA λ^{O}_{max}, the corresponding oscillator strength f, the transition properties, and the corresponding experimental values [16] for the BMVC-I series of molecules are listed in Table 1. The λ^{O}_{max} values obtained using the two methods were very similar, and the λ^{O}_{max} values for the BMVC-I series were also consistent with the experimental values [16, 32]. This indicates that the two methods are suitable for calculating these properties of the studied molecules. Therefore, we calculated the OPA properties of the BMVC and BMVC-C series with the same methods. From Table 1, it is clear that there are two strong OPA peaks for the BMVC series according to both the TDDFT and ZINDO methods, which occur at around 400 nm and 350 nm. Li et al. reported that the λ^{O}_{max} values of the BVC series are about 380nm and 320 nm [32]. These results show that the neutral BMVC molecules exhibit a slight redshift relative to the BVC series due to the introduction of the methyl groups. In addition, there is an obvious redshift for the BMVC-C series relative to BMVC, which may suggest that the N atoms on the 3- and 6-vinylpyridinium groups are important sites. The absorption peaks for the BMVC-C molecules as calculated by the TDDFT method are primarily centered on 440 nm and 530 nm. However, there are other OPA peaks at around 600 nm and 680 nm according to the ZINDO method. For the BMVC-I series, OPA peaks at about 440 nm and 620 nm were found by both the TDDFT and ZINDO methods, and the maximum at 440 nm is in agreement with experimental values [16].

Next, we assigned the transition nature to each main OPA peak. In order to study the transition properties in detail, we drew the contour surfaces of the frontier molecular orbitals related to the OPA properties for the BMVC, BMVC-C, and BMVC-I molecules (see Fig. 2). As shown in Fig. 2 and Table 1, for the main HOMO→LUMO electron transitions in the molecules BMVC1–BMVC3 and the main HOMO→LUMO+2 electron transitions in the molecule BMVC4 in OPA, charge transfer occurs from the 3- and 6-(1-methyl-4-vinylpyridinium) substituents to the central carbazole ring. For BMVC-C molecules, the main transitions with the largest oscillator strengths occur from the HOMO, HOMO-1, and HOMO-4 to the LUMO in the OPA process, respectively, and the main charge transfer occurs from the central ring to the 3- and 6-(1-methyl-4-vinylpyridinium) groups. Accordingly, it also suggested that the N atoms in the 3- and 6-(1-methyl-4-vinylpyridinium) groups are important sites. It is clear from the orbital contours of BMVC-I1, BMVC-I2, and BMVC-I3 and Table 1 their HOMO electron clouds are centralized on the iodine ions of the ends of the molecule (this corresponds to ca. 440 nm in the OPA spectrum). Nevertheless, the electron clouds of the corresponding LUMO are centered on average on the central carbazole ring. For BMVC-I4, the OPA peak at 456 nm corresponds to transitios from HOMO-1 and HOMO-2 to LUMO+3 and LUMO+6, respectively. The electron clouds of HOMO-1 and HOMO-2 are mainly centered on the iodine ions of the ends of the molecule during the OPA process, while the electron clouds of LUMO+3 and LUMO+6 are located in the substituent R4. Thus, this charge transfer must occur from the iodine ions to the R4 group. This may also be caused by the presence of the iodine ions. These results confirm that the N atoms at the 3, 6, and 9 positions are active sites.

Finally, from Table 1, we can also see that the oscillator strengths f gradually increase as the alkyl chain increases from BMVC-I1 to BMVC-I3 (i.e., its value is 0.42 for BMVC-I1, 0.49 for BMVC-I2, and 0.56 for BMVC-I3). This can be ascribed to the increasing electron-donating capability of substituent R upon changing from BMVC-I1 to BMVC-I3. The substituent R4 of BMVC-I4 is an electron-accepting group, Mulliken charge population analysis shows that the charge of R4 beside the iodine ion is 0.73 a.u., while the f value of BMVC-I4 is 0.22. Therefore, we can conclude from the above analysis that the N atoms in the 3- and 6-vinylpyridinium groups are activation sites. Introducing iodine ions to these active sites has a significant effect on the OPA properties of the molecule. On the other hand, there is no obvious change in the OPA properties when the N9 position in the central carbazole ring is substituted with different alkyl groups.

Two-photon absorption properties

In this subsection, the TPA properties of all of the molecules were studied using the ZINDO program in combination with the SOS formulae [21, 24–30] and Eqs. 1 and 2; the accuracy of this approach has already been validated in multiple studies [28, 33–35]. The calculated wavelength of maximum TPA λ^{T}_{max}, the imaginary part of the third-order nonlinear optical susceptibility (Im γ), the maximum TPA cross-section (δ^{T}_{max}), the corresponding transition properties, components, and weights are collected in Table 2. The TPA spectra are plotted in Fig. 3. The contour surfaces of the frontier molecular orbitals related to the TPA properties of each series are shown in Fig. 2. The results indicate that the BVC molecules present TPA cross-sections of <95 GM (1 GM = 10^{-50}cm^4 s photon^{-1}) around

Table 1 One-photon absorption properties of the studied molecules

Molecule	λ^{O}_{max} (nm)			$f_{(ZINDO)}$	Transition nature		
	Exp. [16][a]	TDDFT	ZINDO				
BMVC1		398.9	396.8	1.07	$S_0 \rightarrow S_3$	(HOMO,0) →(LUMO,0)	51.6%
						(HOMO-1,0) →(LUMO+1,0)	20.1%
		346.2	361.8	0.63	$S_0 \rightarrow S_6$	(HOMO-1,0) →(LUMO+1,0)	14.6%
						(HOMO-3,0) →(LUMO,0)	13.0%
						(HOMO-2,0) →(LUMO+2,0)	10.2%
BMVC2		398.7	398.4	1.02	$S_0 \rightarrow S_3$	(HOMO,0) →(LUMO,0)	52.6%
						(HOMO-1,0) →(LUMO+1,0)	20.8%
		349.7	360.5	0.57	$S_0 \rightarrow S_6$	(HOMO-3,0) →(LUMO,0)	16.8%
						(HOMO-1,0) →(LUMO+1,0)	12.9%
						(HOMO,0) →(LUMO,0)	52.4%
BMVC3		398.7	398.0	1.02	$S_0 \rightarrow S_3$	(HUMO-1,0) →(LUMO+1,0)	21.4%
						(HOMO-3,0) →(LUMO,0)	16.9%
		349.9	360.3	0.58	$S_0 \rightarrow S_6$	(HOMO-1,0) →(LUMO+1,0)	12.7%
						(HOMO,0) →(LUMO+2,0)	29.3%
BMVC4		404.3	415.5	1.03	$S_0 \rightarrow S_7$	(HOMO-1,0) →(LUMO+2,0)	21.6%
						(HOMO,0) →(LUMO,0)	15.6%
						(HOMO-1,0) →(LUMO,0)	16.3%
		351.0	376.5	0.56	$S_0 \rightarrow S_{11}$	(HOMO-1,0) →(LUMO,0)	45.1%
BMVC-C1			674.8	1.11	$S_0 \rightarrow S_1$	(HOMO,0) →(LUMO+1,0)	30.1%
						(HOMO,0) →(LUMO,0)	41.6%
			601.7	0.49	$S_0 \rightarrow S_2$	(HOMO-1,0) →(LUMO+1,0)	37.6%
						(HOMO-1,0) →(LUMO+6,0)	17.0%
		515.5	516.8	0.02	$S_0 \rightarrow S_3$	(HOMO-2,0) →(LUMO,0)	16.8%
						(HOMO,0) →(LUMO+6,0)	28.7%
		438.6	410.8	0.11	$S_0 \rightarrow S_6$	(HOMO,0) →(LUMO+1,0)	27.8%
BMVC-C2			689.0	1.12	$S_0 \rightarrow S_1$	(HOMO,0) →(LUMO,0)	46.4%
						(HOMO-1,0) →(LUMO+1,0)	29.0%
			608.5	0.51	$S_0 \rightarrow S_2$	(HOMO-1,0) →(LUMO,0)	39.9%
						(HOMO,0) →(LUMO+1,0)	38.6%
		538.7	521.7	0.02	$S_0 \rightarrow S_3$	(HOMO,0) →(LUMO+6,0)	17.5%
						(HOMO-2,0) →(LUMO,0)	16.6%
		442.2	412.5	0.11	$S_0 \rightarrow S_6$	(HOMO-1,0) →(LUMO+6,0)	29.4%
						(HOMO-1,0) →(LUMO+1,0)	26.6%
BMVC-C3			691.2	1.12	$S_0 \rightarrow S_1$	(HOMO,0) →(LUMO,0)	46.4%
						(HOMO-1,0) →(LUMO+1,0)	29.0%
			609.6	0.51	$S_0 \rightarrow S_2$	(HOMO-1,0) →(LUMO+1,0)	41.0%
						(HOMO,0) →(LUMO+1,0)	38.6%
		543.8	522.0	0.02	$S_0 \rightarrow S_3$	(HOMO,0) →(LUMO+6,0)	17.5%
						(HOMO-2,0) →(LUMO,0)	16.7%
		443.4	412.7	0.11	$S_0 \rightarrow S_6$	(HOMO,0) →(LUMO+7,0)	29.9%
						(HOMO-1,0) →(LUMO+1,0)	26.3%
BMVC-C4			665.6	1.00	$S_0 \rightarrow S_2$	(HOMO-4,0) →(LUMO,0)	34.0%
						(HOMO-3,0) →(LUMO+1,0)	30.4%
		550.3	580.8	0.36	$S_0 \rightarrow S_5$	(HOMO-3,0) →(LUMO+1,0)	25.2%
						(HOMO-2,0) →(LUMO+5,0)	24.2%
						(HOMO-4,0) →(LUMO,0)	21.1%
		455.4	405.6	0.08	$S_0 \rightarrow S_{16}$	(HOMO-3,0) →(LUMO+7,0)	23.8%

Table 1 (continued)

Molecule	λ^{O}_{max} (nm)			f (ZINDO)	Transition nature		
	Exp. [16][a]	TDDFT	ZINDO				
						(HOMO-4,0) →(LUMO+1,0)	19.4%
BMVC-I1		612.1	620.6	0.50 0.18[b]	$S_0 \rightarrow S_3$	(HOMO-1,0) →(LUMO,0)	60.3%
	452.0	437.0	438.0	0.42 0.63[b]	$S_0 \rightarrow S_9$	(HOMO,0)→(LUMO+1,0)	17.1%
BMVC-I2	458.0	612.6	623.7	0.51	$S_0 \rightarrow S_3$	(HOMO,0)→(LUMO+1,0)	61.4%
				0.18[b]		(HOMO-1,0)→(LUMO,0)	16.0%
		447.0	440.7	0.49	$S_0 \rightarrow S_9$	(HOMO-1,0)→(LUMO+2,0)	16.4%
				0.44 [b]		(HOMO-3,0)→(LUMO,0)	16.2%
BMVC-I3		618.3	636.3	0.48	$S_0 \rightarrow S_3$	(HOMO,0)→(LUMO+1,0)	61.6%
				0.14 [b]		(HOMO-1,0)→(LUMO,0)	15.6%
	462.0	450.3	443.5	0.56	$S_0 \rightarrow S_9$	(HOMO-3,0)→(LUMO,0)	20.4%
				0.44 [b]		(HOMO-1,0)→(LUMO+2,0)	11.2%
BMVC-I4		646.5	676.7	0.57	$S_0 \rightarrow S_1$	(HOMO-1,0)→(LUMO,0)	75.8%
				0.24 [b]		(HOMO-1,HOMO-1)→(LUMO,LUMO)	12.4%
			546.7	0.67	$S_0 \rightarrow S_3$	(HOMO-2,0)→(LUMO+1,0)	32.0%
						(HOMO,0)→(LUMO+2,0)	26.0%
						(HOMO-10,0)→(LUMO+1,0)	15.3%
	454.0	442.4	456.3	0.22	$S_0 \rightarrow S_{12}$	(HOMO-2,0)→(LUMO+3,0)	41.1%
				0.63 [b]		(HOMO-1,0)→(LUMO+6,0)	11.6%

[a] Experimental values obtained in ethanol

[b] Corresponding oscillator strength at the TDDFT level

λ^{O}_{max} wavelength of maximum OPA

f corresponding oscillator strength at the ZINDO level

Transition nature transition component and weight

BVC 3,6-bis(4-vinylpyridinium) carbazole

BMVC 3,6-bis(1-methyl-4-vinylpyridinium) carbazole

BMVC-C 3,6-bis(1-methyl-4-vinylpyridinium) carbazole dication

BMVC-I diiodized 3,6-bis(1-methyl-4-vinylpyridinium) carbazole

640 nm. The TPA peaks of BMVC molecules all occur around 615 nm, but δ^{T}_{max} is significantly greater for BMVC compared to BVC (about threefold). We can conclude that introducing the alkyl groups into the 3- and 6-vinylpyridinium groups and at the 9 position of BVC can affect the TPA cross-section. The transitions corresponding to λ^{T}_{max} are $S_0 \rightarrow S_{13}$ and $S_0 \rightarrow S_{21}$, and mainly involve HOMO→LUMO+2 and HOMO→LUMO+9 transitions. It can be seen from the HOMO and LUMO+2 contour plots of BMVC1–BMVC3 that the electron transfer mainly occurs from the 3- and 6-(1-methyl-4-vinylpyridinium) groups to the central carbazole ring during the TPA process. For BMVC4, the main transitions occur from HOMO to LUMO+9. The value of δ^{T}_{max} is 604.7 GM, which is larger than those for BVC and BMVC1–BMVC3. The electron density of LUMO+9 of BMVC4 is concentrated on the central carbazole ring at the 9 position, which is obviously different from the LUMO locations of BMVC1–BMVC3. This result shows that introducing the iodine ion into molecules is an efficient way to enlarge the TPA cross-section. This again confirms that the N atoms of the vinylpyridinium groups are active sites. The values of λ^{T}_{max} for the BMVC-C series are located at around 1200 nm, in the long near-infrared region, so they are obviously redshifted relative to those of BVC and BMVC molecules. The δ^{T}_{max} values for the BMVC-C series are about five times larger than those of BVC molecules, and about 150 GM larger than those of the BMVC molecules. The δ^{T}_{max} values of BMVC-C1, BMVC-C2, and BMVC-C3 gradually increase as the electron-donating capability of the substituent increases. The transitions corresponding to their maximal

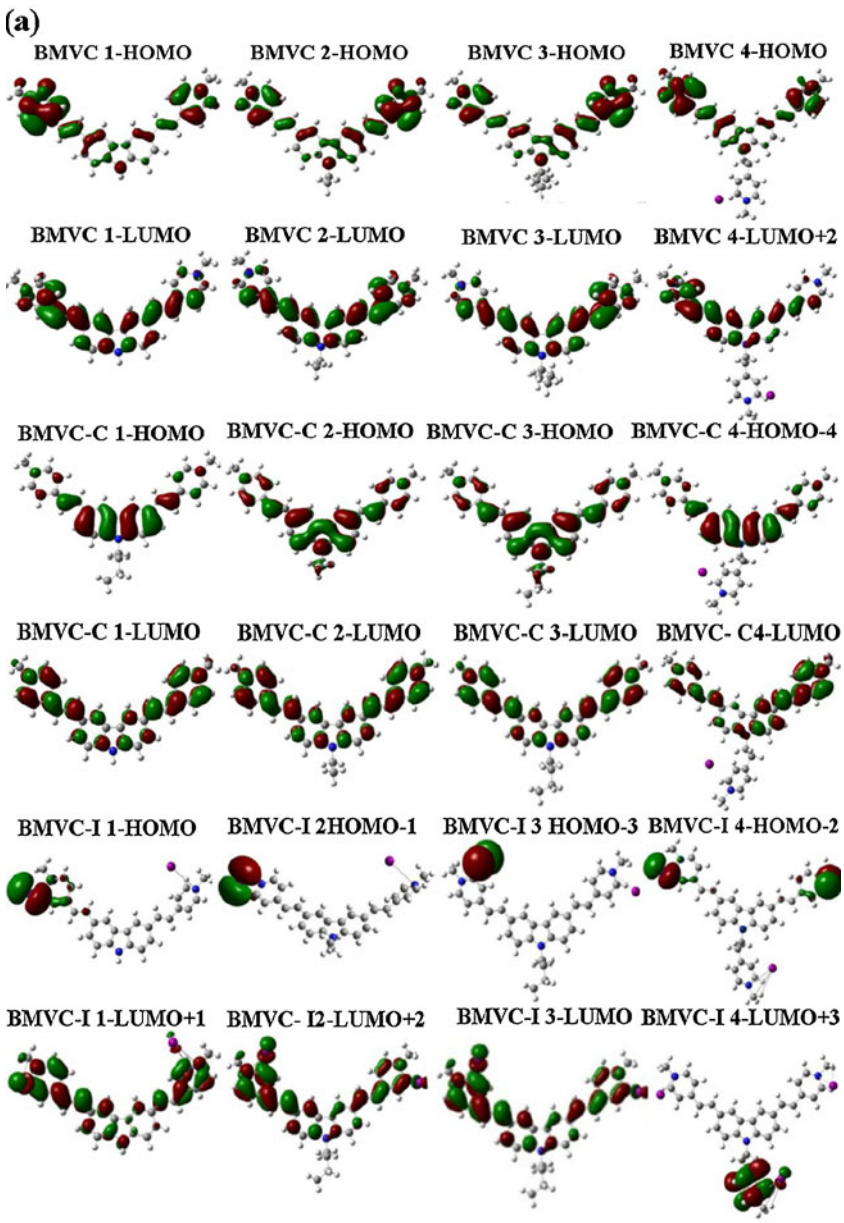

Fig. 2 Contour surfaces of the frontier orbitals relevant to OPA and TPA for the studied molecules. **a** Contour surfaces of the frontier orbitals relevant to OPA. **b** Contour surfaces of the frontier orbitals relevant to TPA

TPA cross-section values δ^{T}_{max} are the low-energy transitions $S_0 \rightarrow S_2$, and mainly comprise HOMO→LUMO and HOMO-1→LUMO transitions. In the TPA process, the electron clouds of the HOMOs are distributed mainly on the central carbazole ring, while the LUMOs are mainly localized on the 3- and 6-(1-methyl-vinylpyridinium) groups. BMVC-C4, with an electron-accepting group as the substituent R_4, has the smallest δ^{T}_{max} value in the BMVC-C series, and the transition corresponding to δ^{T}_{max} is the low-energy transition $S_0 \rightarrow S_6$, relating to HOMO-2→LUMO+5. The electron cloud distribution changes from the substituent R_4 to the 3,6-bis(4-vinylpyridinium) carbazole. The λ^{T}_{max} values of the BMVC-I series are redshifted relative to those of the BVC and BMVC series. The δ^{T}_{max} values of the BMVC-I series decrease in the order BMVC-I3 > BMVC-I2 > BMVC-I1 > BMVC-I4, indicating that the δ^{T}_{max} values increase with the electron-donating capability of the substituent. Due to its electron-accepting substituent, the δ^{T}_{max} value of BMVC-I4 is smaller than those of other molecules. The δ^{T}_{max} values of the BMVC-I series are 7–10 times larger than those of the BVC series, about three times larger than those of the BMVC series, and twice as large as those of the BMVC-C series. In summary, the cation and iodized forms of the molecules have enhanced δ values compared to the others.

Fig. 2 (continued)

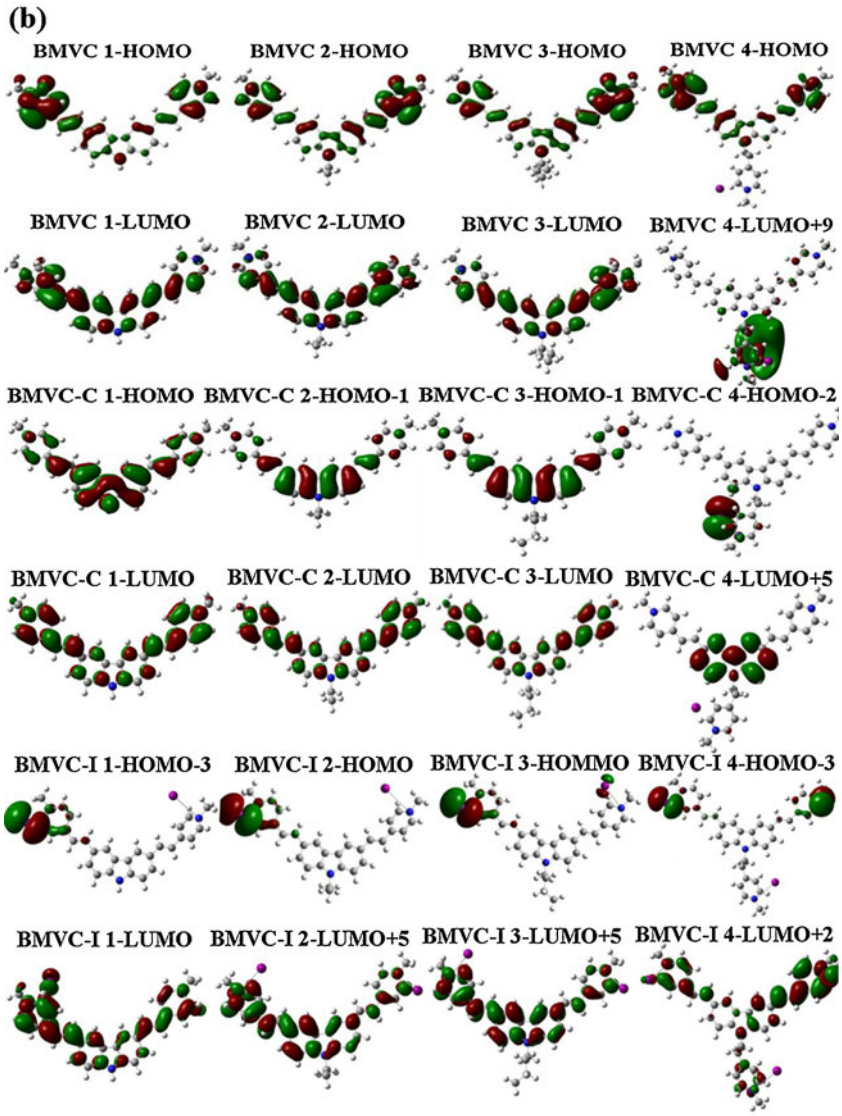

The NLO response is closely related to the bond length alternation (BLA) [36, 37], which is defined as the average difference in length between the single and double bonds in the molecule. We calculated the BLA values of the BMVC-I molecules and compared the behavior of the TPA cross-section and BLA for the molecules studied. As shown in Table 3, the results indicate that BLA increases in the order BMVC-I3 < BMVC-I2 < BMVC-I1 < BMVC-I4, BMVC-I3 < BMVC-C3 < BMVC3, while δ^{T}_{max} decreases in the order BMVC-I3 > BMVC-I2 > BMVC-I1 > BMVC-I4 and BMVC-I3 > BMVC-C3 > BMVC3. This indicates that the smaller the BLA, the more conjugated the molecule, and consequently the larger the TPA cross-section. In conclusion, BMVC-I molecules have small BLA values, meaning that BMVC-I molecules possess large δ^{T}_{max} values as well as λ^{T}_{max} values in the near-infrared region.

Conclusions

In the paper, we theoretically investigated the geometric structures, electronic structures, and the one- and two-photon absorption properties of neutral molecules and cations of 3,6-bis(4-vinylpyridinium) carbazole derivatives. The calculated results indicate that the vinylpyridinium groups at the 3 and 6 positions of the carbazole and the N in each vinylpyridinium group are all active sites, and changing the substituent at the active site has a great effect on the TPA properties (including

Table 2 Two-photon absorption properties of the studied compounds

Molecule	$\lambda_{max}{}^{T}$ (nm)	Im γ (10^{-34} esu)	δ_{max}^{T} (GM)	Transition nature		
BVC1	635.2	1854.4	76.0	$S_0 \rightarrow S_4$	(HOMO,0)→(LUMO+1,0)	54.8%
					(HOMO-1,0)→(LUMO,0)	34.8%
BVC2	641.2	2367.4	95.2	$S_0 \rightarrow S_4$	(HOMO,0)→(LUMO+1,0)	57.8%
					(HOMO-1,0)→(LUMO,0)	31.4%
BVC3	637.6	2083.2	84.3	$S_0 \rightarrow S_4$	(HOMO,0)→(LUMO+1,0)	56.3%
					(HOMO-1,0)→(LUMO,0)	32.5%
BMVC1	613.8	5702.0	249.7	$S_0 \rightarrow S_{13}$	(HOMO,0)→(LUMO+2,0)	22.2%
					(HOMO-2,0)→(LUMO+5,0)	10.1%
BMVC2	617.5	4796.9	207.5	$S_0 \rightarrow S_{13}$	(HOMO,0)→(LUMO+2,0)	20.7%
					(HOMO-2,0)→(LUMO+5,0)	10.2%
BMVC3	617.5	4733.4	204.8	$S_0 \rightarrow S_{13}$	(HOMO,0)→(LUMO+2,0)	21.5%
BMVC4	615.6	13894.0	604.7	$S_0 \rightarrow S_{21}$	(HOMO,0)→(LUMO+9,0)	17.4%
					(HOMO,0)→(LUMO+10,0)	15.7%
BMVC-C1	1203.7	28830.7	328.2	$S_0 \rightarrow S_2$	(HOMO,0)→(LUMO,0)	41.6%
					(HOMO-1,0)→(LUMO+1,0)	37.6%
BMVC-C2	1217.9	31975.4	355.6	$S_0 \rightarrow S_2$	(HOMO-1,0)→(LUMO,0)	41.0%
					(HOMO,0)→(LUMO+1,0)	38.6%
BMVC-C3	1217.9	32176.1	357.8	$S_0 \rightarrow S_2$	(HOMO-1,0)→(LUMO,0)	41.0%
					(HOMO,0)→(LUMO+1,0)	38.6%
BMVC-C4	1156.6	26337.2	324.8	$S_0 \rightarrow S_6$	(HOMO-2,0)→(LUMO+5,0)	61.0%
					(HOMO-3,0)→(LUMO+1,0)	12.4%
BMVC-I1	844.6	23055.0	533.1 [550][a]	$S_0 \rightarrow S_{12}$	(HOMO-3,0)→(LUMO,0)	24.5%
BMVC-I2	851.5	32151.0	731.3 [670][a]	$S_0 \rightarrow S_{10}$	(HOMO,0)→(LUMO+5,0)	26.4%
					(HOMO,0)→(LUMO+2,0)	18.9%
BMVC-I3	858.6	38651.6	864.7	$S_0 \rightarrow S_{10}$	(HOMO,0)→(LUMO+5,0)	28.2%
					(HOMO-1,0)→(LUMO+2,0)	12.7%
BMVC-I4	851.5	23727.8	531.7	$S_0 \rightarrow S_{16}$	(HOMO-3,0)→(LUMO+2,0)	25.9%
					(HOMO-4,0)→(LUMO,0)	18.4%

1 GM = 10^{-50} cm^4 s $photon^{-1}$

[a] Experimental values obtained in ethanol [16]

λ_{max}^{T} wavelength of maximum TPA

Im γ imaginary part of the third-order nonlinear optical susceptibility

δ_{max}^{T} maximum TPA cross-section

Transition nature transition component and weight

BVC 3,6-bis(4-vinylpyridinium) carbazole

BMVC 3,6-bis(1-methyl-4-vinylpyridinium) carbazole

BMVC-C 3,6-bis(1-methyl-4-vinylpyridinium) carbazole dication

BMVC-I diiodized 3,6-bis(1-methyl-4-vinylpyridinium) carbazole

the TPA spectra) of the molecule. Introducing iodine ions into the studied molecule also clearly changed the TPA cross-section values. In addition, the BLA investigation of BMVC-I suggested that BLA decreases as the electron-donating capability of the substituent at the N9 position increases. The more conjugated the molecule, the larger the TPA cross-section. The BMVC-C and BMVC-I molecules were found to have large TPA cross-sections in the NIR region, which makes them promising NIR two-photon imaging materials. In summary, the 3, 6, and 9 positions are the active sites when the studied molecules interact with DNA as two-photon fluorescent probes. Combining neutral molecules with DNA

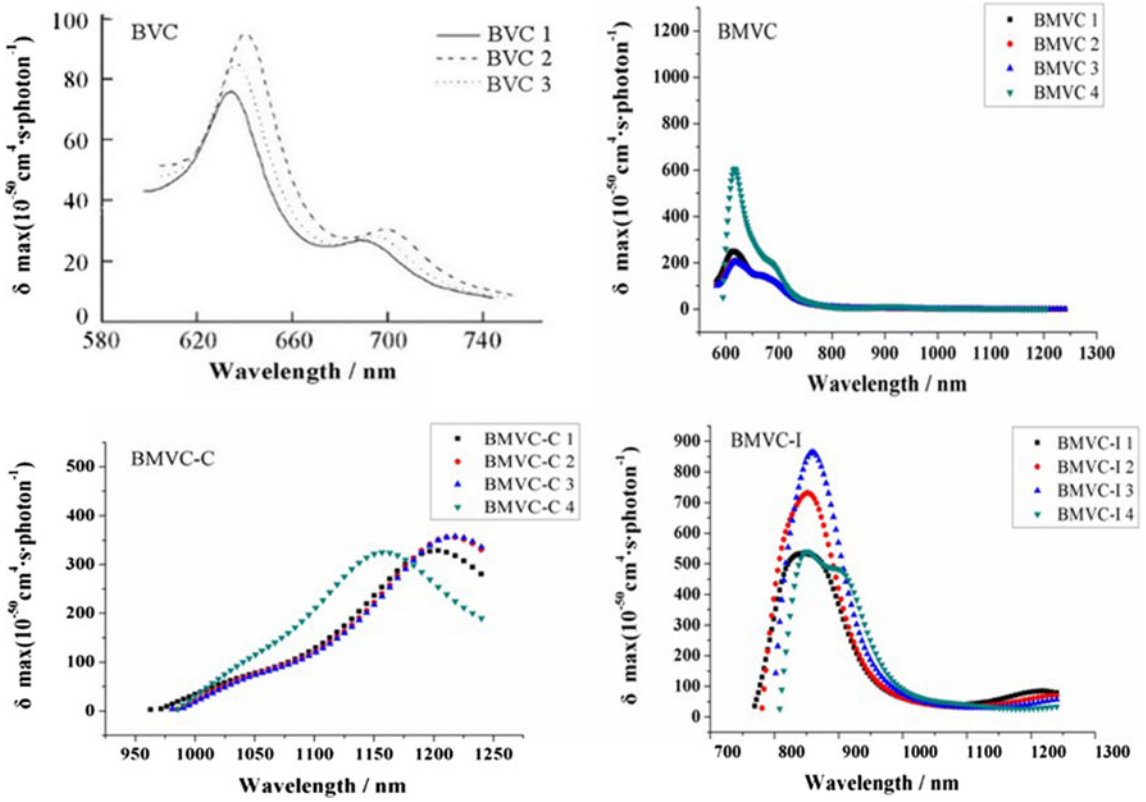

Fig. 3 Two-photon absorption spectra of the molecules studied. The spectrum of BVC is from [31]. BVC: 3,6-bis(4-vinylpyridinium) carbazole. BMVC: 3,6-bis(1-methyl-4-vinylpyridinium) carbazole. BMVC-C: 3,6-bis(1-methyl-4-vinylpyridinium) carbazole dication. BMVC-I: diiodized 3,6-bis(1-methyl-4-vinylpyridinium) carbazole

will not produce DNA "light switch" effects. Among the molecules studied, the BMVC-C and BMVC-I molecules are most likely to combine with DNA as TFPs. Further studies revealed that introducing another ion at the N positions of the 3- and 6-vinylpyridinium groups can enhance the TPA cross-section.

Table 3 Differences between the average lengths of single and double bonds for various molecules

Molecule	Sum of all single bond lengths (Å)	Average single bond length (Å)	Sum of all double bond lengths (Å)	Average double bond length (Å)	BLA[a] (Å)
BMVC-I1	24.0829	1.4166	19.4014	1.3858	0.0308
BMVC-I2	24.0784	1.4164	19.4061	1.3862	0.0302
BMVC-I3	24.0753	1.4162	19.4087	1.3863	0.0299
BMVC-I4	24.0861	1.4168	19.4026	1.3859	0.0309
BMVC-C3	23.9566	1.4092	16.6754	1.3472	0.0620
BMVC3	29.3192	1.4660	17.9534	1.3810	0.0850

[a] Difference between the average length of a single bond and that of a double bond

BMVC-I diiodized 3,6-bis(1-methyl-4-vinylpyridinium) carbazole

BMVC-C 3,6-bis(1-methyl-4-vinylpyridinium) carbazole dication

BMVC 3,6-bis(1-methyl-4-vinylpyridinium) carbazole

Acknowledgments This work is supported by the Natural Science Foundation of China (nos. 21173099, 20973078, and 20673045), as well as the Open Project of the State Key Laboratory for Superamolecular Structure and Material of Jilin University (SKLSSM200716).

References

1. Dvornikov AS, Rentzepis PM (1995) Opt Commun 119:341–346
2. Cumpston BH, Ananthavel SP, Barlow S, Dyer DL, Ehrlich JE, Erskine LL, Heikal AA, Kuebler SM, Lee IYS, McCord-Maughon D, Qin JQ, Rockel H, Rumi M, Wu XL, Marder SR, Perry JW (1999) Nature 398:51–54
3. Denk W, Svoboda K (1997) Neuron 18:351–357
4. Allain C, Schmidt F, Latia R, Bordeau G, Fiorini-Debuisschert C, Charra F, Tauc P, Teulade-Fichou MP (2007) Chem Biochem 8:424–433
5. Ehrlich JE, Wu XL, Lee IYS, Hu ZY, Röckel H, Marder SR, Perry JW (1997) Opt Lett 22:1843–1845
6. Fleitz PA, Sutherland RA, Strogkendl FP, Larson FP, Dalton LR (1998) SPIE Proc 3472:91–97
7. Bhawalkar JD, He GS, Prasad PN (1996) Rep Prog Phys 59:1041–1070
8. Bhawalkar JD, Kumar ND, Zhao CF, Prasad PN (1997) J Clin Laser Med Surg 15:201–204
9. König KJ (2000) Microscopy 200:83–104
10. Zipfel WR, Williams RM, Christie R, Nikitin AY, Hyman BT, Webb WW (2003) Proc Natl Acad Sci USA 100:7075–7080
11. Köhler RH, Cao J, Zipfel WR, Webb WW, Hanson MR (1997) Science 276:2039–2042
12. Miller MJ, Wei SH, Parker I, Cahalan MD (2002) Science 296:1869–1873
13. Helmchen F, Denk W (2005) Nat Methods 2:932–940
14. Zipfel WR, Williams RM, Webb WW (2003) Nat Biotechnol 21:1369–1377
15. Kim HM, Jung C, Kim BR, Jung SY, Hong JH, Ko YG, Lee KJ, Cho BR (2007) Angew Chem Int Edn 46:3460–3463
16. Zhang YH, Wang JJ, Jia PF, Yu XQ, Liu H, Liu X, Zhao N, Huang BB (2010) Org Biomol Chem 8:4582–4588
17. Cha M, Torruellas WE, Stegeman GI, Horsthuis WHG, Mohlmann GR, Meth J (1994) Appl Phys Lett 65:2648–2650
18. Kogej T, Beljonne D, Meyers F, Perry JW, Marder SR, Bredas JL (1998) Chem Phys Lett 298:1–6
19. Bishop DM, Luis JM, Kirtman BJ (2002) Chem Phys 116:9729–9739
20. Orr BJ, Ward JF (1971) Mol Phys 20:513–526
21. Tsuzuki S, Katoh R, Mikami M (2008) Mol Phys 106:1621–1629
22. Frisch MJ, Trucks GW, Schlegel HB, Scuseria GE, Robb MA, Cheeseman JR, Montgomery JA Jr, Vreven T, Kudin KN, Burant JC, Millam JM, Iyengar SS, Tomasi J, Barone V, Mennucci B, Cossi M, Scalmani G, Rega N, Petersson GA, Nakatsuji H, Hada M, Ehara M, Toyota K, Fukuda R, Hasegawa J, Ishida M, Nakajima T, Honda Y, Kitao O, Nakai H, Klene M, Li X, Knox JE, Hratchian HP, Cross JB, Adamo C, Jaramillo J, Gomperts R, Stratmann RE, Yazyev O, Austin AJ, Cammi R, Pomelli C, Ochterski JW, Ayala PY, Morokuma K, Voth GA, Salvador P, Dannenberg JJ, Zakrzewski VG, Dapprich S, Daniels AD, Strain MC, Farkas O, Malick DK, Rabuck AD, Raghavachari K, Foresman JB, Ortiz JV, Cui Q, Baboul AG, Clifford S, Cioslowski J, Stefanov BB, Liu G, Liashenko A, Piskorz P, Komaromi I, Martin RL, Fox DJ, Keith T, Ai-Laham MA, Peng CY, Nanayakkara A, Challacombe M, Gill PMW, Johnson B, Chen W, Wong MW, Gonzalez C, Pople JA (2003) Gaussian 03, revision B.01. Gaussian Inc, Pittsburgh PA
23. Ridley J, Zerner M (1973) Theor Chim Acta 32:111–134
24. Albota M, Beljonne D, Brédas JL, Heikal AA, Hess ST, Kogej T, Levin MD, Marder SR, McCord-Maughon D, Perry JW, Rockel H, Rumi M, Subramaniam G, Webb WW, Wu XL, Xu C (1998) Science 281:1653–1656
25. Peng Q, Niu YL, Wang ZH, Jiang YQ, Li Y, Liu YJ, Shuai ZG (2011) J Chem Phys 134:074510
26. Linnanto J, Freiberg A, Korppi-Tommola J (2011) J Phys Chem B 115:5536–5544
27. Ren AM, Feng JK, Guo JF (2001) Acta Chim Sinica 59:508–515
28. Zhou X, Ren AM, Feng JK (2004) Chem Eur J 10:5623–5631
29. Zhou X, Feng JK, Ren AM (2005) Chem Phys Lett 403:7–15
30. Geskin VM, Lambert C, Bredas JL (2003) J Am Chem Soc 125:15651–15658
31. Li WC, Feng JK, Ren AM, Sun JZ, Yu XQ, Wang JJ (2010) Chem J Chinese Univ 1:100–105
32. Liu X, Liu H, Jia PF, Zhang B, Wang JJ, Zhao N, Zhang YH, Yu XQ (2009) Chem J Chinese Univ 3:465–467
33. Zhao Y, Ren AM, Feng JK, Sun CC (2008) J Chem Phys 129:014301
34. Zhao Y, Ren AM, Feng JK, Zhou X, Ai XC, Su WJ (2009) Phys Chem Chem Phys 11:11538–11545
35. Zhou X, Ren AM, Feng JK, Liu XJ, Zhang YD (2003) Chem Phys Chem 4:991–997
36. Marder SR, Perry JW, Bourhill G, Gorman CB, Tiemann BG, Mansour K (1993) Science 261:186–189
37. Murugan NA, Kongsted J, Rinkevicius Z, Ågren H (2010) Proc Natl Acad Sci USA 107:16453–16458